Wave manipulation with designer dielectric metasurfaces

Jierong Cheng, Davood Ansari-Oghol-Beig, and Hossein Mosallaei*

Department of Electrical and Computer Engineering, Northeastern University, 360 Huntington Ave., Boston, Massachusetts 02115, USA

**Corresponding author: hosseinm@ece.neu.edu*

Received August 18, 2014; revised September 28, 2014; accepted September 29, 2014; posted October 7, 2014 (Doc. ID 221058); published October 27, 2014

The concept of an ultra-thin metasurface made of single layer of only-dielectric disks for successful phase control over a full range is demonstrated. Conduction loss is avoided compared to its plasmonic counterpart. The interaction of the Mie resonances of the first two modes of the dielectric particles, magnetic and electric dipoles, is tailored by the dimensions of the disks, providing required phase shift for the transmitted beam from 0° to 360°, together with high transmission efficiency. The successful performance of a beam-tilting array and a large-scale lens functioning at 195 THz demonstrates the ability of the dielectric metasurface that is thin and has also high efficiency of more than 80%. Such configurations can serve as outstanding alternatives for plasmonic metasurfaces especially that it can be a scalable design.

OCIS codes: (160.3918) Metamaterials; (260.5740) Resonance; (290.4020) Mie theory; (050.5080) Phase shift.

http://dx.doi.org/10.1364/OL.39.006285

Metamaterials and especially metasurfaces have attracted significant interests in the optics community. The central idea is the engineering of metal and dielectric inclusions in fashions to provide novel physics [1–3]. At the beginning stages of the metamaterial design evolution, the focus was mainly on the realization of 3D bulk metamaterials. However, there has been a recent shift of interest toward 2D and layered metasurfaces [4,5], particularly since they exhibit higher potential for fabrication.

The study of optical metamaterials was perhaps initially motivated with the study of metallic elements and their plasmonic properties. However, in order to avoid the inherently high-level losses at optical frequencies and to increase the feasibility of fabrication, comprehensive studies were conducted on dielectric-only metamaterials using Mie resonances [6,7]; starting with a dielectric resonator, electric and magnetic dipole modes are excited and interfered in specifically designed architecture to realize all-dielectric metamaterials [8].

With respect to the Mie series, electromagnetic modes excited in a dielectric particle (spheres are considered here for the sake of simplicity in theory) can be expressed as electric dipole, magnetic dipole, and higher order multi-pole terms with different mode coefficients. The lowest order mode is usually associated with a magnetic dipole mode, and the second one is often associated with an electric dipole mode. It is quite interesting to bring electric and magnetic resonances around the same frequency band, so that effective permittivity and permeability can be tailored together provided that the building block is small enough to realize homogenized equivalent-material parameters. Many interesting designs can be established based on this simple concept. For instance, double-negative (DNG) all-dielectric metamaterials are developed at frequencies above the two (electric and magnetic) resonances [8]. Furthermore, zero backscattering was initially predicated in the dielectric sphere as a result of the mutual interference of the two resonances [9], and then successfully demonstrated at optical frequencies in experiments [10,11]. Perfect absorbing metasurface made of all-dielectric particles has also been reported recently [12].

There are several ways to engineer the above mentioned Mie resonances. One possible way is to use two particles of different sizes or different materials combined in a building block, so that one generates the electric dipole moment, and the other generates the magnetic dipole moment [8]. Another favorable way is to use only one particle in each building block. We also illustrated in our earlier study [13,14] that tailoring the couplings between elements can properly engineer and merge the electric and magnetic modes to the desired directions. Our study here shows by fine tuning the response of the dielectric resonator around the overlap of the electric and magnetic resonances, impedance matching and a wide range of transmission-phase variation can be fulfilled at the same time. Thus the method can be used as a unique means to manipulating beam phase via controlling the resonance and coupling, while maintaining a negligible level of losses.

The use of plasmonic elements in realization of beam phase control has been reported in various works [15,16]. Nonetheless, almost all of the designs suffer from Ohmic losses while a complete 360° phase coverage also necessities the cascading of multiple layers, thus increasing fabrication complexity and cost. The focus of this Letter is to implement the concept of metasurfaces with dielectrics. Only one layer of dielectric elements with an approximate thickness of $\lambda_0/6$ is enough to control both electric and magnetic resonances and to manage the required phase change. The configuration can in fact establish a Huygens' metasurface, as it can successfully manage both electric (J) and magnetic (M) currents in sub-wavelength scale in order to tailor the wave-front as desired. We will focus on elliptical or circular dielectric disk inclusions as they can provide a better control on wave manipulation compared to spheres. We have recently noted a related work [17]. But here we study elliptical disk and more importantly we will provide a full wave simulation of the whole all-dielectric metasurface configuration for beam bending and focusing for the first time to clearly address all the couplings and to prove the idea.

We study first how magnetic and electric resonant modes can be achieved and controlled in periodic lattice

of elliptical disks as one modifies the dimensions of the disks. The resonator disk used here is made of silicon with permittivity of $\varepsilon_r = 12.25$ embedded in a background media of $\varepsilon_r = 2.25$, i.e., SiO_2. As shown in Fig. 1(a), a square lattice with a lattice constants of $\Lambda = 900$ nm is used for the design. The thickness of the disk is fixed to $h = 250$ nm in this work. The diameter of the elliptical disk along $x(y)$ direction is denoted by $a(b)$, and both a and b are used as control parameters for tuning to the desired electromagnetic response. The transmission through an infinite single-layer lattice of the disks is obtained by finite-difference time-domain (FDTD) simulation. A plane wave excitation with $\vec{k} = k_z\hat{z}$ and $\vec{E} = E_y\hat{y}$ polarization is used. Figure 1(b) shows the transmission amplitude for silicon disk with $a = 300$ nm and $b = 340$ nm. The first two resonances are observed at $f_1 = 211.7$ THz and $f_2 = 214.6$ THz. The mode analysis in Fig. 1(c) shows that the first mode profile is a magnetic dipole resonance, and the second is an electric dipole resonance. Such mode distribution is similar to the case of spheres, as the aspect ratio of the disk is close to 1. As the study in [10] shows, increasing the diameter of the disk will gradually merge the two resonances together, where total transmission and impedance matching can be achieved. Further increase of the dimensions of the disk will switch the positions of the two resonances, where electric dipole becomes the dominant mode. This can be explained since the two modes move with different paces as the diameters of the disk increases. Note that the electric resonance is highly influenced by the coupling between neighboring disks, while the magnetic resonance is mainly due to the circular displacement current inside the disk. Thus, the electric resonance exhibits a quicker shift with the change of a and b while the magnetic resonance is only slightly affected.

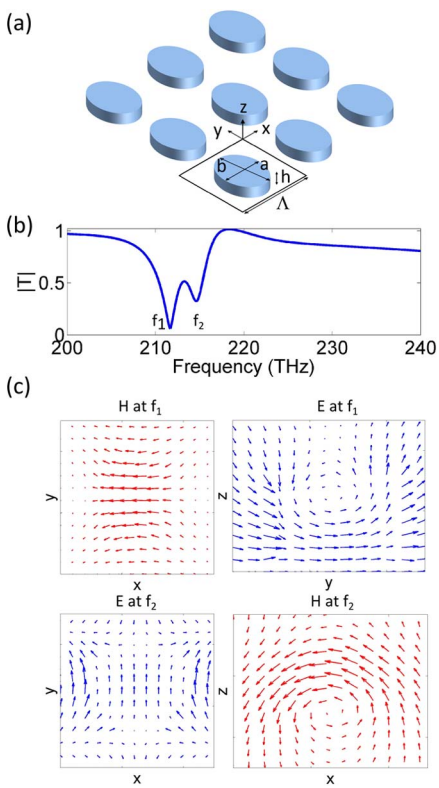

Fig. 1. (a) Elliptical disk array made of Si embedded in SiO_2. (b) Transmission amplitude for periodic disks with $a = 300$ nm and $b = 340$ nm. (c) Field profiles at the two resonances clearly show creation of magnetic dipole mode at f_1 and electric dipole mode at f_2.

The transmission phase and amplitude of the elliptical disk lattice as functions of a and b (at $f = 195$ THz) is systematically studied in Fig. 2. Here, the operating frequency of $f = 195$ THz is a fixed frequency in the overlap of electric and magnetic resonances of the disk. As seen from Fig. 2, complete (360°) transmission-phase coverage is achieved by proper choice of the disk diameters while maintaining a transmission amplitude of $|T| > 0.7$ almost over the entire 360° phase cycle. The magnetic and electric resonances are properly tailored and coupled to give the total phase coverage. In Fig. 2, by looking at the area around the diagonal of the plots (i.e., when the disks are circular), one observes a smooth phase transition of 360° while maintaining a transmission amplitude of $|T| > 0.9$. Thus we identify the circular-shaped building blocks as good candidates for the design of high-efficiency polarization-insensitive metasurfaces. It is needless to say that the elliptical disks find application in scenarios with a requirement for polarization control or polarization sensitive phase control. In addition, the elliptical disks provide more flexibility in the choice of the dimensions compared to the circular ones, thus relaxing the resolution requirement and easing the fabrication constraints.

Figure 2 can then serve as the design chart for various beam engineering synthesis using the designer dielectric-disk building blocks. As a demonstration, example metasurfaces for beam bending and focusing are considered and presented below at 195 THz. Due to the low dispersion property of the all-dielectric material, it works quite well at any other frequencies by scaling the dimensions of the disk. Note here the building block is not in

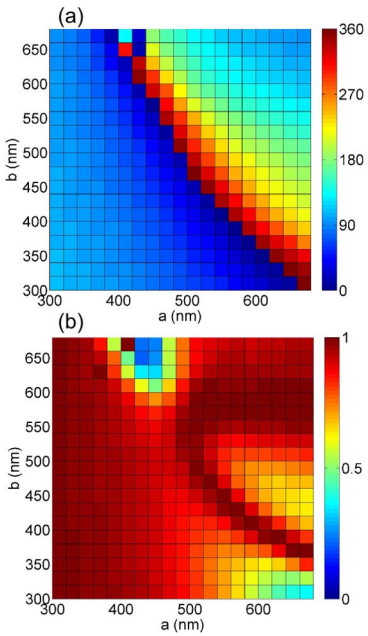

Fig. 2. Variation of the transmission phase (a) and amplitude (b) with a and b of the elliptical disk, where 360° phase change is fully covered.

the sub-wavelength scale, which is usually the case for plasmonic metasurfaces. But it still works the same way to tailor the wave-front except that the phase variation from one cell to a neighboring cell should be sufficiently slow in order to satisfy the local periodicity assumption within the metasurface array. It is worth mentioning that the concept of all-dielectric metasurface is not based on periodicity, rather upon the electric and magnetic modes creation in the disks. One can design smaller size building blocks using higher-index dielectrics, but this seems to be an impractical task (at least for now).

As a general design rule, one first has to discretize the transmission phase as fixed values in the range of [0°, 360°] using a fixed step size of 10° (for example). Next, the associated building blocks, i.e., the geometric parameters a and b for each phase step, is determined by looking up the data in Fig. 2. Clearly, one may encounter situations with multiple choices of disk dimensions for a given phase. For isotropic designs, the choices along the diagonal ($a = b$) should be considered. For anisotropic designs, however, the choice of a and b should avoid the two corner areas where the building blocks exhibit extreme anisotropy and higher losses. Next, the required phase distribution $\Phi(x, y)$ is discretized with the 10° resolution. Then the 36 types of elements are arranged accordingly to compose the metasurface array for the desired beam phase manipulation.

A metasurface for beam bending of $\theta = 9°$ in y–z plane is shown in Fig. 3. The computer model used for this simulation is an infinite array of dielectric disks with uniform pattern along x direction and gradient pattern along y direction. The phase change between immediately neighboring building blocks (along y) is calculated as

$$\Delta\Phi = k_{\mathrm{SiO}_2}\,\Lambda\,\sin(\theta) = 51.4°, \tag{1}$$

where k_{SiO_2} is the wave number in the SiO_2 background while the unit cell size Λ equals to 900 nm. Since the phase cycle is repeated every 360°, the array pattern repeats along y in cycles of 7 building blocks. Within one cycle, the phase change is discretized into {0°, 50°, 100°, 150°, 210°, 260°, 310°}. The building block dimensions corresponding to these 7 phase steps are listed in Table 1 and schematically displayed in Fig. 3(a). The FDTD simulation result depicted in Fig. 3(b) indicates that the normally incident plane wave (of amplitude $|E^{\mathrm{inc}}| = 1.$) is tilted by 7° as it passed through the single-layer array of dielectric disks. It is noteworthy that the amplitude of the tilted beam is around 0.82, validating the proclaimed low losses of the dielectric array design. The discontinuity of the wave-front is observed around $a = b = 500$ nm due to the deviation from the local periodicity assumption, as the phase response is most sensitive to the change of the disk dimensions around that region. Actually the imperfection of the performance highlights the merit of full-wave simulation, from which one can predict the real implementation considering all the couplings.

To further illustrate the flexibility of all-dielectric metasurfaces, a much larger metasurface lens antenna is designed with 27×27 elements sitting in the x–y plane. The phase profile of a general lens is specified as

$$\Phi(x, y) = k_{\mathrm{SiO}_2}\left(\sqrt{x^2 + y^2 + f^2} - f\right). \tag{2}$$

In this case, a focal length f is designed to be 45λ, where λ is the wavelength in the background SiO_2, leading to f/D (D is the diameter of the lens) of 1.9. The required phase for each element is calculated from Eq. (2) and discretized with 10° resolution. Next, with the aid of Fig. 2, the dimensions of all of the required building blocks are obtained in Fig. 4 ($a = b$ is considered here). By putting a dipole at the designed focal point and calculating the field distribution before and after the lens, the spherical phase front is modified into the perfect plane phase as

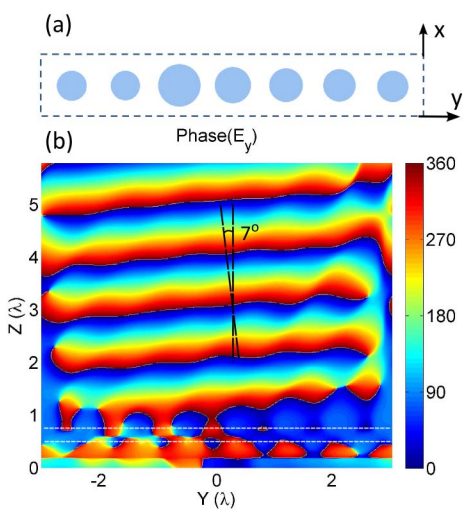

Fig. 3. (a) Super cell in the periodic array for beam tilt. It repeats with a period of 6.3 μm along y and 900 nm along x. (b) Phase of E_y when the plane wave propagating through the dielectric metasurface for beam tilt. The single layer of disks is sitting in the area bounded by two dash white lines.

Table 1. Dimensions of Disks in a Super Cell for Beam Tilt

Cell	1	2	3	4	5	6	7
Phase (°)	0	50	100	150	210	260	310
a (nm)	480	470	680	580	540	520	500
b (nm)	480	470	680	580	540	520	500

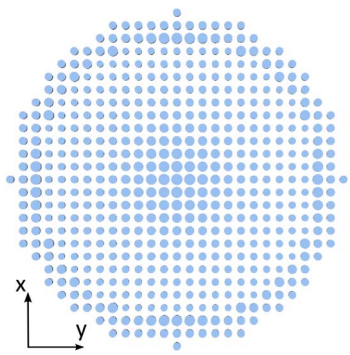

Fig. 4. Structure of the flat lens antenna with 27×27 cells along the diameter and the focal length of 45λ.

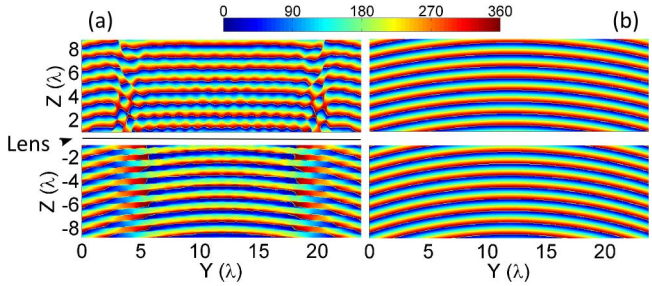

Fig. 5. Full-wave simulation of the evolution of a point-source in front of the lens. (a) Phase of H_x before and after the lens where the lens is a solid black line. (b) Phase of H_x without the lens to compare. The spherical wave is transformed to an almost uniform phase-front plane wave.

reflected in Fig. 5. The 5 cells at the edges have failed to exhibit the desired function due to edge effects and violation of the local periodicity assumption. Note, that the phase changes very rapidly in the area toward the edges. Further examination reveals that the number of functioning building blocks in the vicinity of the lens edges depends on the f/D ratio of the lens. For example, for $f/D = 2.7$, only the two building block in the vicinity of the edges are not functioning as expected. One way to reduce the f/D without facing this problem is to reduce the lattice size Λ. This can be achieved by increasing the material contrast between the background media and the disks. Although the design here is in IR, the concept is scalable and has potential to be implemented in visible band as well.

For the beam tilt array, the periodicity is built into the computer model, hence dramatically reducing the problem size and allowing for the use of our FDTD solver. However, for the metasurface lens, such simplification is not possible. Direct solution of 27×27 array may not be possible using the FDTD solver. Instead, we use in-house array integral equation fast Fourier transform (AIEFFT) solver [18] to model the complete array and to calculate the field distribution before and after the lens. This is critically important as all couplings are taken into account accurately and the full wave phenomenon is studied. The AIEFFT solver is a hybrid accelerated surface integral equation method especially designed for fast solution of large array structures. The computer model for the lens discussed here involves 1.4 million unknowns and the iterative solution of the final linear equation converged to error tolerance of 10^{-4} in 79 iterations.

The bandwidth performance of the dielectric metasurface is discussed here. The phase response follows the nonlinear "S" shape with frequency, where the phase changes rapidly around the resonance and slowly off the resonance. Transmission amplitude has a relatively wide band characteristic. For the designs proposed in this work, one can overall achieve desired behaviors for frequency range from 190 to 205 THz. It must be mentioned that in compared to Fresnel zone plate, the designer dielectric element has the ability to control amplitude and phase cell-by-cell, locally and desirably, not by the zones as is the case for the zone plate. This can offer remarkable design flexibility.

To conclude, the concept of a very thin dielectric metasurface composed of a single layer of dielectric disk array is proposed to enable beam manipulation in IR, which can be readily scaled up to visible range due to the low dispersion nature of the dielectric. Two specific applications as light bending and collimation are presented. They show no Ohmic loss, have high transmission efficiency and full-phase coverage with a single layer. They can also be designed for polarization manipulation utilizing elliptical disks. Such designs can be easily realized on the commercial SOI wafer using the traditional top-down nanofabrication technique as presented in [17]. The merits of low loss, high efficiency, single-layer thin thickness, and frequency scalability (IR to visible) make the designer dielectric concept a unique paradigm for developing novel metasurface applications.

This work is supported by the U.S. Air Force Office of Scientific Research (AFOSR), #FA9550-14-1-0349.

References

1. N. Engheta and R. W. Ziolkowski, *Metamaterials: Physics and Engineering Explorations* (Wiley, 2006).
2. Y. Liu and X. Zhang, Chem. Soc. Rev. **40**, 2494 (2011).
3. N. I. Zheludev and Y. S. Kivshar, Nat. Mater. **11**, 917 (2012).
4. N. Yu and F. Capasso, Nature **13**, 139 (2014).
5. A. V. Kildishev, A. Boltasseva, and V. M. Shalaev, Science **339**, 1232009 (2013).
6. J. A. Stratton, *Electromagnetic Theory* (McGraw-Hill, 1941).
7. Q. Zhao, J. Zhou, F. Zhang, and D. Lippens, Mater. Today **12** (12), 60 (2009).
8. A. Ahmadi and H. Mosallaei, Phys. Rev. B **77**, 045104 (2008).
9. M. Kerker, D.-S. Wang, and C. L. Giles, J. Opt. Soc. Am. **73**, 765 (1983).
10. I. Staude, A. E. Miroshnichenko, M. Decker, N. T. Fofang, S. Liu, E. Gonzales, J. Dominguez, T. S. Luk, D. N. Neshev, I. Brener, and Y. Kivshar, ACS Nano **7**, 7824 (2013).
11. Y. H. Fu, A. I. Kuznetsov, A. E. Miroshnichenko, Y. F. Yu, and B. Luk'yanchuk, Nat. Commun. **4**, 1527 (2013).
12. X. Liu, Q. Zhao, C. Lan, and J. Zhou, Appl. Phys. Lett. **103**, 031910 (2013).
13. S. Ghadarghadr and H. Mosallaei, IEEE Trans. Nanotechnol. **8**, 582 (2009).
14. H. Mosallaei and S. Ghadarghadr, "Electric and magnetic dipole modes analysis of 3D array of two spheres unit cell configuration," *URSI-USNC National Radio Science Meeting*, January 3–6, 2008.
15. B. Memarzadeh and H. Mosallaei, Opt. Lett. **36**, 2569 (2011).
16. J. Cheng and H. Mosallaei, Opt. Lett. **39**, 2719 (2014).
17. M. Decker, I. Staude, M. Falkner, J. Dominguez, D. N. Neshev, I. Brener, T. Pertsch, and Y. S. Kivshar, arXiv: 1405.5038.
18. D. Ansari Oghol Beig and H. Mosallaei, "Array IEFFT solver for simulation of supercells and aperiodic penetrable metamaterials," J. Comput. Phys., submitted for publication.